High-tech alloys based on Al – Ca – La(–Mn) eutectic system for casting, metal forming and selective laser melting

T. K. Akopyan, *Dr., Research Worker of Department of Metal Forming*[1], *e-mail: nemiroffandtor@yandex.ru.*
N.V. Letyagin, *PhD, Engineer of Department of Metal Forming*[1]
N. N. Avxentieva, *Senior Lecturer of the Department Mathematics*[1]

[1] *National University of Science and Technology MISiS, Moscow, Russia.*

Electron microscopy structure studies have shown that new Al3Ca2La(1–2)Mn system alloys have a fine hypoeutectic structure. The fine eutectic fibers are a few microns in length and less than one micron in thickness. EMPA shows that calcium and lanthanum are completely included in the eutectic, while manganese is distributed between the aluminum solid solution (Al) and the eutectic. The solubility of manganese in (Al) is about 1.7 wt.%. Addition of 2 wt.% Mn leads to a substantial increase in the yield strength and ultimate tensile strength of the base Al3Ca2La alloy whereas the ductility is not less than 5%. The yield strength of the quaternary alloy is about 175 MPa which is three times that of the base alloy. Due to the narrow solidification range and a high fraction of eutectic, new Al – (3–6)Ca – (2–4)La – (1–2)Mn alloys also have a lower hot tearing tendency comparable to that of the branded hypoeutectic and hypereutectic Al – Si alloys. The ball-milled experimental powder has been used for a preliminary analysis of the effect of selective laser melting on the as-built microstructure of the model hypereutectic alloy. No cracks and porosity have been observed, the microstructure consisting of very fine eutectic. The microhardness of the as-processed alloy is about 170 HV which is comparable with the hardness of high-strength aluminum alloys. Thus, based on the analysis above, new alloys can be considered as promising for conventional casting and SLM technique instead of the widely used Al – Si alloys. The Al3Ca2La1Mn alloy has also been deformed by radial shear rolling. Hot rolling at 400 °C at a total pulling rate of μ = 8.16 has yielded high-quality 14 mm diameter rods. Microstructure analysis has shown that deformation leads to additional refining of eutectic crystals the average size of which is at a submicron level (300–500 nm). The combination of size of fine eutectic particles and their high volume fraction (~15%) allows reaching good mechanical properties, i.e., an ultimate strength of at least 230 MPa at a relative elongation of at least 15%. Thus the achieved combination of the properties of the new Al – Ca – La(–Mn) alloys allows classing them as high-tech materials suitable for advanced hybrid forming technologies.

Key words: Al-alloys, Al – Ca alloys, eutectic, casting, selective laser melting, radial shear rolling, microstructure, mechanical properties

DOI: 10.17580/nfm.2020.01.09

Introduction

Additive technologies are among the most rapidly developing materials processing trends in Russia and abroad. The cooling rate of the molten powder layer during selective laser melting (SLM) can exceed 10^5 K/s which allows achieving a significant deviation from the equilibrium state and obtaining an ultrafine microstructure with unique parameters [1–2]. SLM process can have general application for the production of aluminum-matrix composites. In particular, great interest is drawn to the study of eutectic compositions (e.g. Al – Si casting alloys [3–5]) due to their low hot tearing tendency during casting and SLM processing. However Al – Si alloys have low as-cast strength and are not suitable for the fabrication of semi-finished products with high reduction rates. These drawbacks restrict the use of Al – Si alloys in the fabrication of complex structures with the use of hybrid technologies. Hybrid technologies combine the advantages of additive, subtractive (lathing, drilling, cutting etc.) and conventional metallurgical technologies (casting and pressure shaping) [6–7]. This combination of different technologies allows fabricating complex shaped metallic products (bionically and topologically optimized configurations allow minimizing product weight) with a unique complex of physical and mechanical properties that are not attainable with sole conventional metallurgical technologies. On the other hand multiple calcium containing aluminum alloys on the basis of ternary and quaternary eutectic systems have been recently studied (Al – Ca – *X*, Al – Ca – Sc – *X* и Al – Ca – *X* – *Y* (where *X* and *Y* are Mg, Zn, Cu, Si, Fe, Ni, Zr and Mn)) [8–15]. Calcium containing eutectic alloys proved to have fine-grained structure and to be prone to changing shape during deformation heat treatment. Most of the simulating calcium containing alloys studied are high-tech materials both for casting and deformation and combine low density, high corrosion resistance and good mechanical properties.

Hypoeutectic alloys of the Al – Ca – La are among the most promising aluminum calcium alloys for hybrid technologies [16]. It was shown that alloys near the ternary eutectic point can contain up to 25 vol.% ultra-fine eutectic intermetallic particles 50–100 nm in thickness and up to 100–400 nm in length. In addition, the Al3Ca2La alloy is effectively hardened by small additions of zirconium and scandium due to the formation of $L1_2$ – (Al_3(Zr,Sc)) phase nanoparticles. Despite these advantages the alloy

has moderate strength (UTS is about 220 MPa) in the as-cast and as-annealed states. This figure is lower than that of heat-treatable Al – Si alloys. An additional increase in the strength of the new alloy can be attained by manganese alloying [17–20]. The maximum solubility of manganese in aluminum (~2 wt.%) determines its maximum content in the aluminum alloys. For instance, from the viewpoint of phase equilibria, the optimal concentration of manganese in industrial 3xxx series alloys is about 1.25% [18, 21–22]. During the solidification of 3xxx alloys, most of Mnis in the solid solution, leading to supersaturation of the (Al) solid solution [22]. Strengthening in these alloys is determined by work hardening and solid solution hardening [22–24]. It should also be noted that according to [25] the addition of manganese to the Al –10La alloy has but little effect on the Al+ $Al_{11}La_3$ eutectic structure while leading to a remarkable improvement of the mechanical properties at room temperature and elevated temperatures (up to 300 °C).

The fine-grained structure of the eutectic alloy also shows good promise for high technological properties of the Al3Ca2La alloy in the fabrication of deformed semi-finishedproducts. The radial shear rolling method [26–29] which allows fabricating round-shaped rolled products is considered as one of the most promising methods of fabricating deformed semi-finished products with a unique combination of mechanical properties. The trajectory-controlled radial shear rolling method has become the most widely used. It provides high shift deformation to refine the metal structure to a submicron size. Radial shear rolling allows producing a gradient structure with fine recrystallized grains near the specimen surface and heavier deformed grains in the center. This structure provides for high strength and plasticity of deformed alloys [30–31].

Thus the aim of this work is to study the technological and mechanical properties of the new family of eutectic aluminum alloys of the Al3Ca2La(–Mn) system produced in the form of cast shapes, wrought semi-finished products and laser-sintered powdered specimens.

2. Materials and Methods

The experimental alloys were prepared from high purity aluminum (99.99%) in a graphite crucible using a Nabertherm K 1/13 resistance furnace in an air atmosphere. Aluminum was placed in the crucible, and after its melting the Al – 15%Ca binary master alloy, pure lanthanum (99.9%) and Al – 20%Mn binary master alloy was added to the melt. After melting of the main components the melt was held for 5–10 min for obtaining a homogeneous composition, and the samples were obtained by casting into a cylindrical steel mold (for shaped castings) and into a graphite cylindrical mold with a diameter of 40 mm for ingots for subsequent processing. The actual chemical compositions of the alloys are presented in Table 1.

The microstructure was examined by means of scanning electron microscopy (SEM, TESCAN VEGA 3), electron microprobe analysis (EMPA, OXFORD AZtec) and transmission electron microscopy (TEM, JEM–2100). Polished samples were used for the studies. Mechanical polishing was used, as well as electrolytic polishing, which was carried out at a voltage of 12 V in an electrolyte containing six parts C_2H_5OH, one part $HClO_4$ and one part glycerine. The thin foils for TEM were prepared by ion thinning with a PIPS (Precision Ion Polishing System, Gatan) machine and studied at 160 kV.

Table 1.
Chemical composition of the experimental alloys

No.	Designation	Concentrations, wt.%			
		Al	Ca	La	Mn
1	Al3Ca2La	94.9	3.1	2.0	–
2	Al3Ca2La1.0Mn	93.9	3.7	2.4	0.9
3	Al3Ca2La2.0Mn	92.4	3.4	2.3	1.7
4	Al6Ca4La2.0Mn	88.3	5.9	4.0	1.8

The 40 mm diam. cylindrical pieces were rolled at 400 °C after annealing at 400 °C for 1 h on a radial shear roling mini-mill 14–40 [15] in four passes with a ∅40→∅31→∅24→∅17→∅14 mm setup. The overall drawing ratio was μ = 8.16, the average extrusion per pass being μ_{av} = 1.69.

The hypereutectic alloy No. 4 was selected for additional studies of the effect of various solidification rates on the resulting structure. The medium cooling rate of 40 K/s was reached by pouring molten metal into a 5 mm cylindrical steel mold. In order to reach a relatively high cooling rate of about 100 K/s we poured molten metal onto a cold metallic surface so to obtain a thin plate of less than 1 mm. The highest cooling rate was obtained after selective laser melting produced by using single track technique.

The raw material for the single track experiment was irregular shaped powder produced from experimental alloy No. 4 chips. The as-cast samples were milled on a lathe for producing the chips. The whole 150 g batch was milled into powder using a 4-reel Retsch PM 400 centrifugal planetary ball mill at 300 rpm. The permanent weight ratio between the stainless steel balls and the experimental alloy chips was 10:1. After 10 min of grinding, the resulting powder was sieved so to achieve a less than 100 microns size.

A commercial SLM Solution 280 machine equipped with a 1064 nm wavelength Yb fiber laser with a power of up to 250 W for local melting, a heatable platform and an argon supply system, was used for the single track experiment. Twelve single tracks were obtained at the following processing parameters: a laser power of 170–250 W and a scanning speed of 200–350 mm/s. The Al – Mg alloy building platform was preheated to 100 °C. The thickness of the deposited layer was 100 μm.

The Vickers hardness was determined on a DUROLINE MH-6 installation (load 1N, dwell time 30 s). Room-temperature tensile tests were conducted for as-processed bar specimens on a Zwick Z250 universal testing machine (loading rate 10 mm/min).

To determine the solidification range of the experimental alloys we used direct thermal analysis with a single chromel-alumel thermocouple submerged into the melt and plugged to an AKTAKOM-2006 recording unit.

Qualitative assessment of the hot tearing tendency (HTT) was carried out with a pencil probe [32]. A special mold that could be opened and closed was used for casting seven cylindrical specimens with head parts. The diameter of the head parts was the same for all the specimens (20 mm), whereas the diameter of the cylinders varied from 4 to 16 mm with a 2 mm step. HTT is defined in this case as the maximum diameter of the cylindrical portion of the sample that still does not reveal any cracks. The higher the HTT, the worse the hot cracking performance of the test aluminum alloy.

A thermodynamic calculation with the Thermo-Calc software and the TTAL5 database was conducted beforehand for facilitating the preliminary analysis of the quaternary system.

3. Results and Discussion

3.1. Analysis of the microstructure and mechanical properties of shaped castings

As stated in the Introduction, alloying with up to 2% Mn can provide additional hardening of the alloy. The microstructure of the new quaternary alloy containing up to 2 wt.% Mn in comparison with the base ternary alloy is shown in Fig. 1. As can be seen, no new structural components are detected in the quaternary alloy as compared to the base ternary alloy. Both alloys have a fine hypoeutectic structure. The fine eutectic layers which were liquid during casting separated (Al) solid grains from one another and were also located in the grain boundary junctions. The fine eutectic fibers are a few microns in length and less than one micron in thickness (see TEM structures in Figs. 1*e*, *f*). EMPA shows that all of the calcium and lanthanum are included in the eutectic, while manganese is distributed between the aluminum solid solution (Al) and the eutectic. The measured solubility of manganese in (Al) is about 1.7 wt.% which is close to the maximum value.

Uniaxial tensile test data for the ternary and quaternary alloys at different manganese contents are shown in Table 2. As can be seen, the base alloy has the lowest yield strength which is determined by the yield strength of low-alloy aluminum solid solution. The continuing strain leads to an increase in the strength due to strain hardening. It is well known [18] that intensely deformed zones form in multi-phase aluminum alloys around fine dispersoids during deformation. The density of these deformed zones may be much higher in metal matrix composites which are reinforced with a large volume fraction of dispersoids. The formation of this substructure provides significant strain hardening during deformation. It should be noted that, according to the XRD results, the base alloy contains about 15 vol.% of Al_4(Ca, La) phase and it can thus be attributed to natural metal matrix composites. It should also be pointed out that despite the relatively high fraction of the intermetallic phase the alloy has a significant ductility exceeding 10%.

Addition of 1 wt.% Mn leads to a substantial increase in the yield strength and ultimate tensile strength (Table 2). The yield strength of the quaternary alloy is about twice that of the base alloy. Despite a slight decrease in ductility by max. 10%, strain hardening is still significant, and the ultimate tensile strength reaches more than 200 MPa which is about 70% higher than that for the base alloy. It should be noted that the observed increase in the yield strength is significantly higher than the expected hardening due to the effect of manganese. The origin of this phenomenon can be the formation of fine manganese containing compound precipitates in the eutectic. An in-

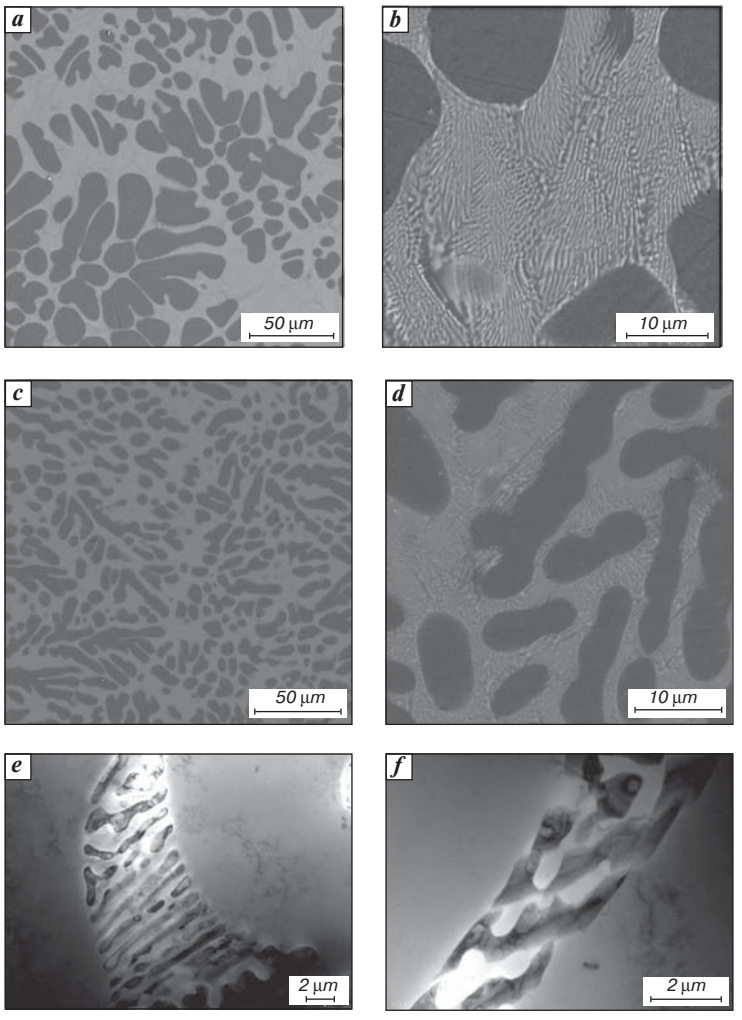

Fig. 1. Microstructure of (*a*, *b*) ternary Al3Ca2La alloy and (*c–f*) quaternary Al3Ca2La2Mn alloy; (*a*, *c*) general view, (*b*, *d–f*) eutectic structure; (*a–d*) SEM, (*e–f*) dark field TEM images

Table 2.
Mechanical properties after uniaxial tensile tests of the Al – Ca – La(–Mn) hypoeutectic alloys

Alloy	No.	UTS, MPa	YS, MPa	δ, %
Al3Ca2La	1	116	57	16.5
	2	123	65	14.1
	3	119	59	8.9
	4	117	68	10.3
Average		119	62	12.5
Al3Ca2La1.0Mn	1	199	112	8.3
	2	212	126	7.5
	3	205	146	13.2
	4	195	127	9.8
Average		203	127	10.7
Al3Ca2La2.0Mn	1	221	180	4.0
	2	234	163	5.6
	3	218	179	6.3
	4	229	173	4.9
Average		225	174	5.2

crease in the fraction of fine unshearable particles should lead to an increase in the yield strength in accordance with the Orowan looping mechanism [33]. However, to confirm this assumption it is also necessary to carry out detailed studies of the quaternary diagram.

A further increase in the concentration of manganese to 2 wt.% leads to an additional increase in yield strength by 35%. The tensile strength increases by only 11% which is associated with a 2-times decrease in the elongation. It should be noted that despite this decrease, the elongation is still sufficient for a ductile material. It should also be stressed that, as shown earlier [16], zirconium and scandium microadditives lead to significant hardening of the alloys after simple annealing. Thus, this feature can also be used for increasing the strength of new quaternary alloys to the level of the branded high-strength Al – Si – Cu alloys after quenching and aging.

As noted above, the new alloys for hybrid technology should possess not only high mechanical properties but also satisfactory manufacturability during casting or SLM production. In our opinion, the hot tearing tendency (HTT) during solidification largely determines the possibility of using the alloy for both the casting or SLM techniques

Qualitative assessment of the hot tearing tendency of the new Al – Ca – La – Mn based alloys in comparison with Al – Si alloys was carried out using a pencil probe [32]. HTT in this case is defined as the minimum diameter of the cylindrical portion of the sample that still does not reveal any cracks. Two alloys based on the promising Al – Ca – La – Mn system were selected for the experiments. One alloy was the above described Al3Ca2La2Mn hypoeutectic alloy and the other one was new Al6Ca4La2Mn hypereutectic alloy the calcium and lanthanum contents in which are near the ternary eutectic point (see Fig. 4*a*.). It should be noted that hypereutectic alloys may have even greater interest in case of SLM technique. It is well known [34–35] that rapid solidification leads to a significant deviation of the solidification path from equilibrium and non-equilibrium conditions. Depending on the thermodynamic factors and kinetic effects [34] defined by a value of under-cooling, formation of a structure corresponding to metastable equilibrium can be expected. Thus, a hypereutectic structure can transform into fully eutectic or hypoeutectic, while transition elements (Mn, Zr, Cr and etc.) form supersaturated solid solutions which can reach about 3 times the maximum equilibrium solid solubility. The formation of such a structure with a high volume fraction of ultra-fine particles homogeneously distributed in a supersaturated aluminum matrix is favorable for achieving a high hardening [35].

To obtain comparative data we also analyzed the Al9Si3Cu based hypoeutectic alloy which is one of the most widely used for the SLM production and the binary Al20Si hypereutectic alloy the silicon content in which is close to the maximum one for industrial aluminum piston alloys. For the analysis of non-equilibrium solidification of the Al – Si based alloys, thermodynamic calculations according to the Scheil-Gulliver model, which is implemented in the Thermo-Calc program [36], have been used. The results (Fig. 2*a*) present a property diagram that shows how

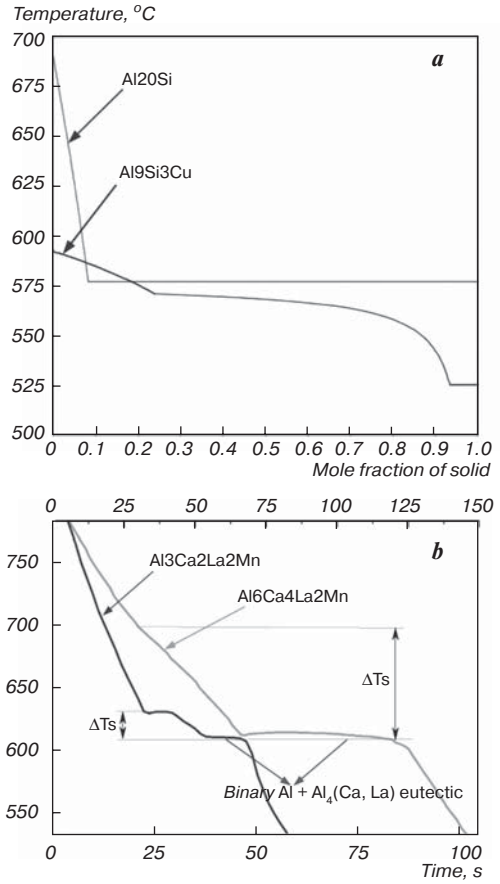

Fig. 2. Non-equilibrium solidification curves calculated for the Al20Si and Al9Si3Cu alloys using the Scheil-Gulliver model simulation (*a*) and experimental cooling curves for the model alloys Al3Ca2La2Mn and Al6Ca4La2Mn (*b*)

the fraction of solid phase varies with temperature during alloy solidification. Since there is no correct thermodynamic description of the new Al – Ca – La system, the solidification of the alloys was analyzed using the direct thermal analysis (Fig. 2*b*). The data obtained are used to determine the non-equilibrium solidification range (ΔTs) of the alloys.

The HTT data for the alloys are presented in Table 3. It can be seen that both hypoeutectic alloys have similar and close to minimum tendencies to form hot cracks. This result agrees well with the general concept of the lower tendency to hot crack formation in alloys having a narrow solidification range [32]. According to the Scheil-Gulliver model simulation, the non-equilibrium solidification range of the Al9Si3Cu alloy is about 55 °C. According to the experimental data, the solidification range of the Al3Ca2La alloy is about 22 °C.

Hypereutectic alloys have higher hot tearing tendency which can be associated with a wider solidification range. In particular, according to the experimental cooling curve, the solidification temperature range of the Al6Ca4La2Mn alloy is about 89 K. General appearance of a hot crack formed during the casting of the Al6Ca4La2Mn alloy is shown in Fig. 3. As can be seen, despite the wider temperature range, the binary Al20Si alloy has a lower tearing tendency (Table 3). However, HTT index of the new alloy is still satisfactory and the superior fraction of the second phases (is about 1.5 times higher than that for the Al20Si alloy) can significantly affect hardening after rapid solidification during SLM production.

Reviewing the results described above, due to the relatively high mechanical properties in the as-cast state, as well as the low hot tearing tendency during solidification, new alloys based on the Al – Ca – La(–Mn) system can potentially be considered promising for the casting production and selective laser melting technique.

3.2. The effect of rapid solidification and SLM on the microstructure of a hypereutectic alloy

As noted above, hypereutectic alloys may have even greater interest in case of SLM production due to the superior fraction of ultra-fine reinforcing second phases formed. Alloy Al6Ca4La2Mn described above was selected for a preliminary analysis of the effect of laser processing on the microstructure of hypereutectic alloys. Before laser processing, the microstructure of the alloy obtained at a medium cooling rate of 40 K/s and after near-rapid solidification at cooling rate of about ~100 K/s has been studied. As can be seen (Fig. 4), in both cases the alloy has a hypereutectic structure. The needle-shaped primary crystals are surrounded by the eutectic. However, in the case of near-rapid solidification, we can observe a much finer structure with a lower fraction of primary intermetallics. Microhardness of as-cast sample obtained at the higher cooling rate is about 10 % higher (110 HV vs 100 HV) due to the finer structure formed.

From a cylindrical ingot with a diameter of 40 mm we produced the chips by using mechanical processing. During further processing in a ball mill, an irregular

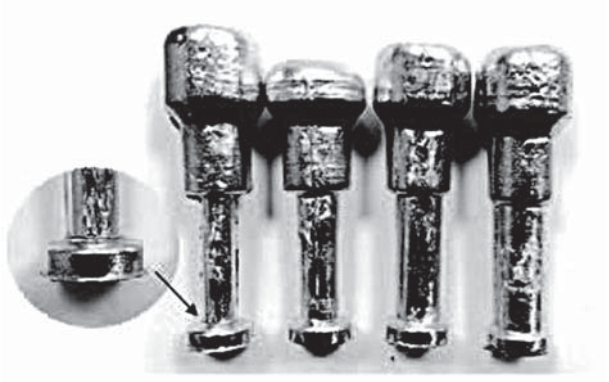

Fig. 3. Cast Al6Ca4La2Mn alloy samples 10 to 16 mm in diameter obtained using the pencil test

Table 3.

Hot tearing tendency of alloys

Alloy	Hot tearing index (minimum diameter of the cast sample, mm)	Non-equilibrium solidification range (ΔTs), °C
Al3Ca2La1.5Mn	4	22
Al9Si3Cu	4	55
Al6Ca4La2Mn	12	89
Al20Si	8	110

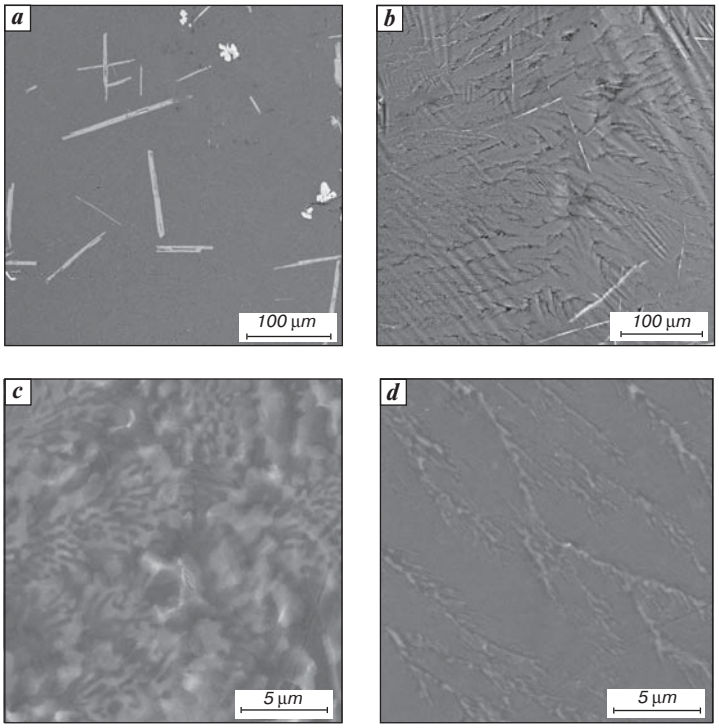

Fig. 4. The microstructure of Al – 6Ca – 4La – 2Mn alloy obtained at cooling rates of (*a*, *c*) 40 K/s and (*b*, *d*) 40 K/s. (*a*, *b*) general view, (*c*, *d*) eutectic structure. SEM

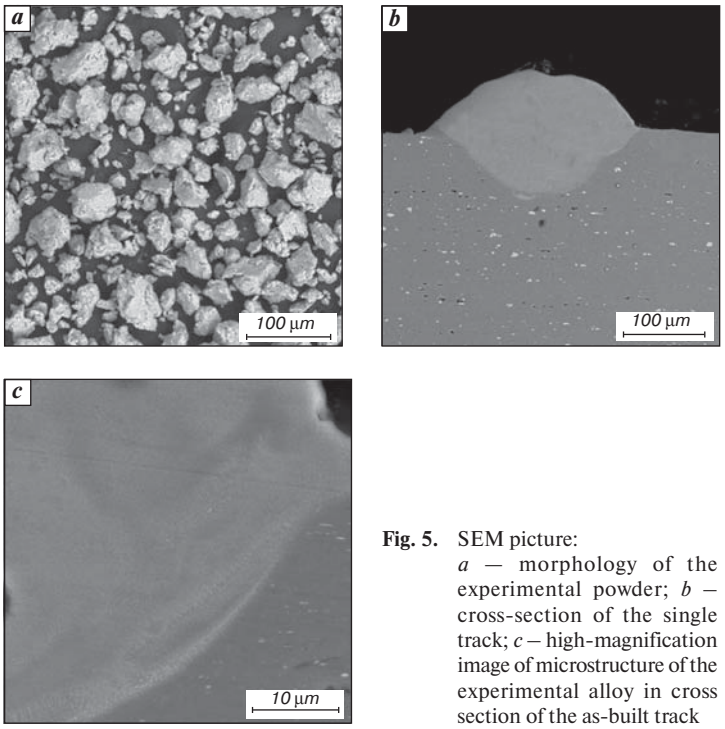

Fig. 5. SEM picture: *a* — morphology of the experimental powder; *b* — cross-section of the single track; *c* — high-magnification image of microstructure of the experimental alloy in cross section of the as-built track

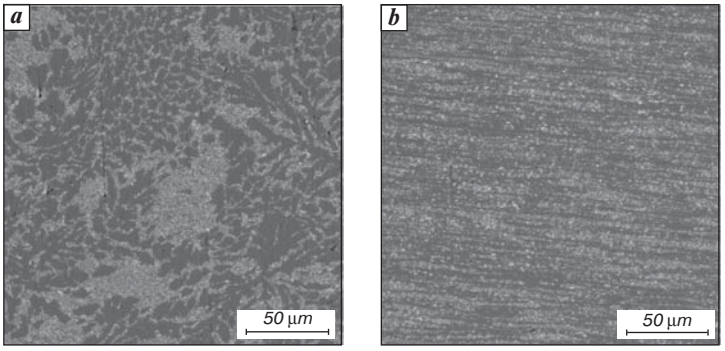

Fig. 6. Microstructure of the Al3Ca2La1Mn alloy after radially shear rolling: *a* — in the cross section; *b* — in the longitudinal section of the 14 mm diam. rod obtained

shape powder with particle size of 20–65 μm was prepared (Fig. 5*a*). Typical cross-section of further obtained single tracks is shown in Fig. 5*b*. No cracks and pores are observed. Fig. 5*c* shows the microstructure of the alloy in cross section of the as-built track. As can be seen, the alloy structure is much finer in comparison with those shown in Fig. 4. A finer eutectic structure is the result of the higher solidification rate during the SLM process. Due to the absence of the primary crystals, the resulting structure can be qualified as quasi-eutectic with the size of individual eutectic intermetallic particles less than 100 μm. The microhardness of the alloy in as-processed state is about 170 HV which is by 52% higher than that for the thin layered sample (cooling rate ~100 K/s).

Thus, based on the analysis of the phase composition, microstructure and mechanical properties, it can be concluded that new alloys based on the Al – Ca – La – Mn system can be considered as promising materials for both conventional casting production and SLM technique instead of the currently used Al – Si alloys.

3.3. Analysis of the microstructure and mechanical properties of wrought semi-finished products

The microstructure of the 14 mm diam. radial shear rolled rod is shown in Fig. 6. During drawingratio radial shear rolling the experimental alloy exhibited high technological properties (hot rolling drawing ratio ~91%) which allowed high-quality 14 mm diam. rods to be fabricated. SEM examination showed (Fig. 6) that radial shear rolling formed a fibrous structure consisting of aluminum grains and eutectic colonies elongated in the rolling direction. High magnification microscopy also allowed evaluating the average grain size. It decreased additionally to submicron sizes (300–500 nm) as a result of rolling.

The combination of the fine-grained structure of eutectic particles and their high volume ratio (~15%) provides for good mechanical properties of the deformed semi-finished products. For example as can be seen from Table 4 the ultimate strength of the allow increases by 17%, the yield stress increases by 30% and the relative elongation increases by 53% in comparison with the as-cast alloy (Table 2). It should be noted that the experimentally observed increase in strength and plasticity of the material after deformation result from eutectic structure refinement and possible formation of a gradient grain structure, but the latter assumption requires additional studies.

Thus our experimental data suggest the good technological properties of the new Al3Ca2La(1–2)Mn alloys for the fabrication of cast shapes and deformed semi-finished products. Preliminary results also confirm the possibility using the new materials for selective laser melting. Analysis of the mechanical properties of the alloys by uniaxial tinsel tests showed that cast products made from the new alloys are not inferior in strength to commercial A356 alloys which require a complete cycle of hardening heat treatment. As-deformed new alloy has the same strength as medium strength alloys (6xxx series) and allows fabricating deformed semi-finished products with high drawing ratio. Thus achieving this combination of properties of the new

Table 4.
Mechanical properties after uniaxial tensile tests of the Al – Ca – La(–Mn) hypoeutectic alloys

Alloy	№	UTS, MPa	YS, MPa	δ, %
Al3Ca2La1.0Mn	1	238	166	16.2
	2	236	163	13.4
	3	240	165	15.6
	4	239	166	16.0
Average		238	165	15.3

alloys allows considering them as promising for fabrication of products using hybrid shaping technologies.

4. Conclusions

1. Structural studies showed that alloys of the new Al3Ca2La(1-2)Mn system have a fine hypoeutectic structure. The fine eutectic fibers are a few microns in length and less than one micron in thickness. Calcium and lanthanum are included in the eutectic, while manganese is distributed between the aluminum solid solution (Al) and the eutectic. Addition of up to 2 wt.% of Mn into the base hypoeutectic Al3Ca2La alloy leads to a 3-fold increase in its yield strength (from 62 to 174 MPa) an dan increase in the ultimate tensile strength by 90 % (from 119 MPa to 225 MPa) while maintaining a high elongation of 5-10%. The hot tearing tendency of the new Al3Ca2La2Mn alloy is not inferior to that of branded Al – Si alloys.

2. Ball milled irregular shape powder from the new Al6Ca4La2Mn hypereutectic alloy was used for analyzing the effect of selective laser melting on microstructure and microhardness. It is shown that single track processed alloy has an ultra-fine quasi-eutectic structure with individual eutectic intermetallic particle sizes of less than 100 μm. The single track cross section had no cracks or pores. The microhardness of the as-processed alloy was about 170 HV which corresponds to the hardness of high-strength aluminum alloys

3. Radial shear rolling of cylindrical shapes from the new Al3Ca2La1Mn alloy at 400 °C with an overall drawing ratio μ = 8.16 produced 14 mm diam. calibrated rods. Analysis of their microstructure shows that radial shear-rolling leads to an additional refinement of the eutectic structural components to submicron average grain sizes (300–500 nm). Uniaxial tensile tests showed that the ultimate strength of the radial shift rolled rods increases by 17%, the yield stress increases by 30% and the relative elongation increases by 53% in comparison with the as-cast state.

Acknowledgements

The study was carried out with the financial support of the grant of the Russian Science Foundation (Project № 18-79-00345).

References

1. Rao H., Giet S., Yang K., Wu X., Davies C. H. J. The Influence of Processing Parameters on Aluminium Alloy A357 Manufactured by Selective Laser Melting. *Materials & Design*. 2016. Vol. 109. pp. 334–346.

2. Tang M., Pistorius P. C., Narra S., Beuth J. L. Rapid Solidification: Selective Laser Melting of AlSi10Mg. *JOM*. 2016. Vol. 68, Iss. 3. pp. 960–966.

3. Leon A., Aghion E. Effect of Surface Roughness on Corrosion Fatigue Performance of AlSi10Mg Alloy Produced by Selective Laser Melting (SLM). *Materials Characterization*. 2017. Vol. 131. pp. 188–194.

4. Jing L., Xu C., Zhuo L., Xiao Z., Shu-Quan Z., Hua-Ming W. Improving the Mechanical Properties of Al – 5Si –1Cu – Mg Aluminum Alloy Produced by Laser Additive Manufacturing with Post-Process Heat Treatments. *Materials Science and Engineering: A*. 2018. Vol. 735. pp. 408–417.

5. Girelli L., Giovagnoli M., Tocci M., Pola A., Fortini A., Merlin M., La Vecchia M. Evaluation of the Impact Behaviour of AlSi10Mg Alloy Produced Using Laser Additive Manufacturing. *Materials Science and Engineering: A*. 2019. Vol. 748. pp. 38–51.

6. Blindheim J., Grong Ø., Welo T., Steinert M. On the Mechanical Integrity of AA6082 3D Structures Deposited by Hybrid Metal Extrusion & Bonding Additive Manufacturing. *Journal of Materials Processing Technology*. 2020. Vol. 282. 116684. DOI: 10.1016/j.jmatprotec.2020.116684

7. Xiang Qiu, Naeem ul Haq Tariq, Lu Qi, Ji-Qiang Wang, Tian-Ying Xiong. A Hybrid Approach to Improve Microstructure and Mechanical Properties of Cold Spray Additively Manufactured A380 Aluminum Composites. *Materials Science and Engineering: A*. 2020. Vol. 772. pp. 138828. DOI: 10.1016/j.msea.2019.138828

8. Belov N. A., Naumova E. A., Akopyan T. K., Doroshenko V. V. Phase Diagram of Al – Ca – Mg – Si System and Its Application for the Design of Aluminum Alloys with High Magnesium Content. *Metals*. 2017. Vol. 7, Iss. 10. pp. 429–445.

9. Jiang Y., Shi X., Bao X., He Y., Huang S., Wu D., Bai W., Liu L., Zhang L. Experimental Investigation and Thermodynamic Assessment of Al–Ca–Ni Ternary System. *Journal of Materials Science*. 2017. Vol. 52, Iss. 20. pp. 12409–12426.

10. Akopyan T. K., Letyagin N. V. Doroshenko V. V. Al – Ca – Ni – Ce-based aluminium matrix composites hardened with L12 phase nanoparticles without quenching. *Tsvetnye Metally*. 2018. No. 12. pp. 56–61. DOI: 10.17580/tsm.2018.12.08

11. Naumova E. A., Akopyan T. K., Letyagin N. V., Vasina M. A. Investigation of the Structure and Properties of Eutectic Alloys of the Al – Ca – Ni System Containing REM. *Non-ferrous Metals*. 2018. No. 2. pp. 24–29. DOI: 10.17580/nfm.2018.02.05

12. Belov N. A., Naumova E. A., Alabin A. N. Matveeva I. A. Effect of Scandium on Structure and Hardening of Al–Ca Eutectic Alloys. *Journal of Alloys and Compounds*. 2015. Vol. 646. pp. 741–747.

13. Belov N. A., Akopyan T. K., Mishurov S. S., Korotkova N. O. Effect of Fe and Si on the Microstructure and Phase Composition of the Aluminum-Calcium Eutectic Alloys. *Non-ferrous Metals*. 2017. No. 2. pp. 37–42. DOI: 10.17580/nfm.2017.02.07

14. Belov N. A., Naumova E. A., Akopyan T. K., Doroshenko V. V. Phase Diagram of the Al–Ca–Fe–Si System and Its Application for the Design of Aluminum Matrix Composites. *JOM*. 2018. Vol. 70, Iss. 11. pp. 2710–2715.

15. Shurkin P. K., Dolbachev A. P., Naumova E. A., Doroshenko V. V. Effect of Iron on the Structure, Hardening and Physical Properties of the Alloys of the Al – Zn – Mg – Ca System. *Tsvetnye Metally*. 2018. No. 5. pp. 69–77. DOI: 10.17580/tsm.2018.05.10

16. Akopyan T. K., Letyagin N. V., Belov N. A., Shurkin P. K. New Eutectic Type Al Alloys Based on the Al – Ca – La(–Zr, Sc) System. *Materials Today: Proceedings*. 2019. Vol. 19. pp. 2009–2012.

17. Hatch J. E. Aluminum: Properties and Physical Metallurgy. American Society for Metals: Ohio, USA, 1984. 363 p.

18. Polmear I. J. Light Alloys From Traditional Alloys to Nanocrystals. Fourth edition. Butterworth-Heinemann. Elsevier: Oxford, UK. 2006. 421 p.

19. Belov N. A., Eskin D. G., Askenov A. A. Multicomponent Phase Diagrams: Applications for Commercial Aluminum Alloys. Elsevier Ltd, Oxford. 2005. 424 p.

20. De Haan P. C. M., Rijkom J. V., Söntgerath J. A. H. The Precipitation Behaviour of High-Purity Al–Mn Alloys. *Materials Science Forum*. 1996. Vol. 217–222. pp. 765–770.

21. Merchant H. D., Morris J. G., Hodgson D. S. Characterization of Intermetallics in Aluminum Alloy 3004. *Materials Characterization*. 1990. Vol. 25, Iss. 4. pp. 339–373.

22. Li Y. J., Arnberg L. Quantitative Study on the Precipitation Behavior of Dispersoids in DC-Cast AA3003 Alloy During Heating and Homogenization. *Acta Materialia*. 2003. Vol. 51, Iss. 12. pp. 3415–3428.

23. Goel D. B., Roorkee U. P., Furrer P., Warlimont H. Precipitation in Aluminum Manganese (Iron, Copper) Alloys. *Aluminium*. 1974. Vol. 50. pp. 511–516.

24. Nicol A. D. I. The Structure of MnAl6. *Acta Crystallographica*.1953. Vol. 6., Iss. 3. pp. 285–293.

25. Alexander D. T. L., Greer A. L. Solid-State Intermetallic Phase Transformations in 3XXX Aluminium Alloys. *Acta Materialia*. 2002. Vol. 50, Iss. 10. pp. 2571–2583.

26. Galkin S. P. Regulating Radial-Shear and Screw Rolling on the Basis of the Metal Trajectory. *Steel in Translation*. 2004. Vol. 34, Iss. 7. pp. 57–60.

27. Diez M., Kim H.-E., Serebryany V., Dobatkin S., Estrin Y. Improving the Mechanical Properties of Pure Magnesium by Three-Roll Planetary Milling. *Materials Science and Engineering: A*. 2014. Vol. 612. pp. 287–292.

28. Stefanik A., Morel A., Mróz S., Szota P. Theoretical and Experimental Analysis of Aluminium Bars Rolling Process in Three-High Skew Rolling Mill. *Archives of Metallurgy and Materials*. 2015. Vol. 60, Iss. 2. pp. 809-813.

29. Lopatin N. V., Salishchev G. A., Galkin S. P. Mathematical Modeling of Radial-Shear Rolling of the VT6 Titanium Alloy under Conditions of Formation of a Globular Structure. *Russian Journal of Non-Ferrous Metals*. 2011. Vol. 52, Iss. 5. pp. 442–447.

30. Lu K. Making Strong Nanomaterials Ductile with Gradients. *Science*. 2014. Vol. 345. pp. 1455–1456.

31. Akopyan T. K., Belov N. A., Aleshchenko A. S., Galkin S. P., Gamin Y. V., Gorshenkov M. V., Cheverikin V. V., Shurkin P. K. Formation of the Gradient Microstructure of a New Al Alloy Based on the Al – Zn – Mg – Fe – Ni System Processed by Radial-Shear Rolling. *Materials Science and Engineering: A*. 2019. Vol. 746. pp. 134–144.

32. Glazoff M. V., Khvan A. V., Zolotorevsky V. S., Belov N. A., Dinsdale A. T. Casting Aluminum Alloys. Their Physical and Mechanical Metallurgy. Oxford, UK : Elsevier, 2019. 564 p.

33. Zhang Z., Chen D. L. Contribution of Orowan Strengthening Effect in Particulate-Reinforced Metal Matrix Nanocomposites. *Materials Science and Engineering: A*. 2008. Vol. 483–484. pp. 148–152.

34. Dobatkin V. I., Elagin V. I., Fedorov V. M. Structure of Rapidly Solidified Aluminum Alloys. *Advanced Performance Materials*. 1995. Vol. 2, Iss. 1. pp. 89–98.

35. Lin Y., Mao S., Yan Z., Zhang Y., Wang L. The enhanced microhardness in a rapidly solidified Al alloy. *Materials Science and Engineering: A*. 2017. Vol. 692. pp. 182–191.

36. Reference Data for Thermodynamic Calculations. Available: http://www.thermocalc.com (accessed: 08.05.2020). NFM